The intimin-like protein FdeC is regulated by H-NS and temperature in Enterohaemorrhagic *Escherichia coli*

Donna M. Easton[1,2], Luke P. Allsopp[1], Minh-Duy Phan[1], Danilo Gomes Moriel[1], Guan Kai Goh[1], Scott A. Beatson[1], Timothy J. Mahony[3], Rowland N. Cobbold[2], Mark A. Schembri[1,#]

[1]*Australian Infectious Disease Research Centre, School of Chemistry and Molecular Biosciences, The University of Queensland, St Lucia, Australia*

[2]*School of Veterinary Science, The University of Queensland, Gatton, Australia*

[3]*Queensland Alliance for Agriculture and Food Innovation, The University of Queensland, St Lucia Australia*

Running title: *FdeC* is regulated by H-NS and temperature in EHEC

Corresponding author.

Mailing address: School of Chemistry and Molecular Biosciences, Building 76, University of Queensland, Brisbane QLD 4072, Australia. Phone: +617 33653306; E-mail: m.schembri@uq.edu.au

Abstract

Enterohaemorrhagic *Escherichia coli* (EHEC) are Shiga toxigenic pathogens capable of inducing severe forms of enteritis (e.g. hemorrhagic colitis) and extraintestinal sequelae (e.g. hemolytic uremic syndrome). The molecular basis of colonization of human and animal hosts by EHEC is not yet completely understood and an improved understanding of EHEC mucosal adherence may lead to development of interventions that could disrupt host colonization. FdeC, also referred to by its IHE 3034 locus tag ECOK1_0290, is an intimin-like protein that was recently shown to contribute to kidney colonisation in a mouse urinary tract infection model. The expression of FdeC is tightly regulated *in vitro*, and FdeC shows promise as a vaccine candidate against extra-intestinal *E. coli* strains. In this study we characterised the prevalence, regulation and function of *fdeC* in EHEC. We showed that the *fdeC* gene is conserved in both O157 and non-O157 EHEC, and encodes a protein that is expressed at the cell surface and promotes biofilm formation under continuous flow conditions in a recombinant *E. coli* strain background. We also identified culture conditions where FdeC is expressed, and showed that minor alterations of these conditions, such as changes in temperature, can significantly alter the level of FdeC expression. Additionally, we demonstrate that the transcription of the *fdeC* gene is repressed by the global regulator H-NS. Taken together, our data suggest a role for FdeC in EHEC when growing at temperatures above 37°C, a condition relevant to its specialized niche at the recto-anal junction of cattle.

Introduction

Enterohemorrhagic *Escherichia coli* (EHEC) are Shiga toxigenic pathogens capable of inducing severe forms of enteritis, such as hemorrhagic colitis (HC), and extraintestinal sequelae, such as haemolytic uremic syndrome (1). Ruminant livestock are the principal hosts of Shiga toxigenic *E. coli* (STEC) (2, 3), including EHEC, where they are often carried at the herd and individual animal level as commensal enteric flora (4). Food-borne transmission of STEC through contamination of primary produce is a significant factor in the epidemiology of EHEC infections that are prevalent world-wide. The O157 serotype is considered the archetypal EHEC, although there are small number of non-O157 serotypes that are more commonly associated with severe disease than other non-O157 serotypes. In the USA, the Food and Drug Administration recently designated six non-O157 serotypes (O26, O45, O103, O111, O121, O145) as food adulterants, highlighting these as being of enhanced public health significance, and increasing the stringency of STEC food safety assurance regulation and testing requirements at a global level (5).

The molecular mechanisms associated with the colonization of human and animal hosts by EHEC are not yet completely understood. Colonization is generally considered to involve three steps: 1) initial attachment, 2) translocation of bacterial components to mammalian cells via a type III secretion system (T3SS), and 3) intimate attachment characterised by the formation of attaching and effacing lesions, and mediated by the bacterial effector intimin (6). Research has focused on the locus for enterocyte effacement (LEE), which encodes a T3SS that is produced by strains of EHEC and closely related enteropathogenic *E. coli* (EPEC), as well as a range of translocated effector molecules. It is likely that other mediators of colonization are yet to be identified, particularly for non-O157 EHEC, and particularly with respect to colonization of bovine hosts. An improved understanding of EHEC

63 mucosal adherence may lead to the development of interventions that could inhibit host colonization.
64 This could provide benefit either by disrupting colonization of humans to prevent the acquisition of
65 such strains leading to disease, or by reducing colonization of livestock and thus decreasing
66 transmission of EHEC to humans via decreases in food contamination. An intimin-based vaccine is
67 already available for the reduction of colonisation of cattle with O157 strains, however no such
68 control measure is available for non-O157 EHEC (7).
69
70 A recently described *E. coli* adhesin, FdeC (GenBank accession ADE88959), contributes to *E. coli*
71 colonisation of the upper urinary tract in a mouse infection model (8). Immunisation with FdeC, also
72 known by its IHE3034 locus tag ECOK1_0290, is also protective in mouse models of urinary tract
73 infection (UTI) and sepsis (8, 9), demonstrating FdeC represents a potential vaccine antigen against
74 uropathogenic *E. coli* (UPEC) mediated UTI. While the expression of FdeC is undetectable under
75 normal laboratory growth conditions, the protein is expressed during co-culture with mammalian cells
76 and *in vivo* (8). FdeC shares structural similarity with intimin, containing an N-terminal β-barrel and C-
77 terminal extracellular domain, and belongs to the type Ve group of autotransporter proteins (10).
78 FdeC was identified in genome sequences from a range of different *E. coli* pathotypes, however to-
79 date has only been studied for its potential role in uropathogenesis.
80
81 In this study we have described conditions under which FdeC is expressed by EHEC and demonstrated
82 that the level of FdeC expression can be manipulated by minor alteration of these conditions. We
83 have also shown that expression of FdeC is repressed by the global regulator H-NS (11) and that FdeC
84 mediates biofilm formation following over-expression in a recombinant strain under continuous flow

85 conditions. Taken together, our data imply a potential role for FdeC in colonisation of the terminal
86 rectum of cattle.
87

Methods

Strains and growth conditions. N39 (also known as EC673) is an *eae* and *stx1* positive, O26:H11 strain of *E. coli* originally isolated from faeces of an Australian calf. EDL933 is a well-characterized O157:H7 EHEC outbreak isolate (12). *E. coli* MS427 (K12 strain MG1655Δ*flu*; i.e. lacks Ag43) and OS56 (green fluorescent protein [GFP]-tagged MG1655Δ*flu*) have been described previously (13-15). Plasmid pHNS has been described previously (16). Cells were grown at 37°C on solid or in liquid Luria–Bertani (LB) media supplemented with the appropriate antibiotics (100 μg/ml ampicillin, 50 μg/ml kanamycin) unless otherwise stated. Where necessary, gene expression was induced with 1 mM IPTG.

DNA manipulations and genetic techniques. Genomic DNA was extracted from overnight cultures using the Wizard® Genomic DNA Purification Kit (Promega, Madison, WI, USA) following the manufacturer's procedure for Gram-negative bacteria. Plasmid DNA was isolated using the QIAprep Spin Miniprep Kit (Qiagen, Germantown, MD, USA) following the manufacturer's instructions. Restriction digests, ligations, and T4 polymerase treatment followed the manufacturer's recommendations (New England BioLabs, Ipswich, MA, USA). PCR reactions for which high fidelity was required were performed using Expand High Fidelity Polymerase System (Roche, Basel, Switzerland) following the manufacturer's recommendations. Taq DNA polymerase (New England BioLabs) was used for screening PCR reactions. DNA sequencing was performed by the Australian Equine Genetics Research Centre.

Construction of plasmids. The *fdeC* gene was amplified by PCR from N39 with primers designed using the available genome sequence of O26:H11 strain 11368 (3018 5'-GGCGAGCTCCATCAGGAAATTATCTCAATGTCA and 3019 5'-GGCAAGCTTAAATTATTTCATCGCCTCCTCGTC). The PCR product was digested with *Sac*I (forward primer) and *Hin*dIII (reverse primer) and ligated to *Sac*I–*Hin*dIII digested plasmid pSU2718 (17) to generate plasmid pFdeC. In this construct, the transcription of *fdeC* was under the control of the IPTG-inducible *lac* promoter.

Antiserum production and immunoblotting. A 6×histidine-tagged 97 kDa truncated form of FdeC was constructed. Primers 2871 (5′-TACTTCCAATCCAATGCGCTTGACGGTCAGAGCCGTAT) and 2830 (5′-TTATCCACTTCCAATGTTAGTTCATCGCCTCCTCGCCCT) were used to amplify the portion of the gene coding for the predicted extracellular component of the protein (amino acids 467-1417), which was then inserted into the pMCSG7 vector by ligation-independent cloning and maintained in *E. coli* DH5α (18). This plasmid was then transferred to *E. coli* BL21 for expression of the recombinant protein by induction with 1 mM IPTG and purification by Ni-NTA Superflow columns (Qiagen) under native conditions (following the manufacturer's instructions). Protein purity was assessed by SDS-PAGE analysis as previously described (19). Polyclonal anti-FdeC serum was raised in rabbits by the Institute of Medical and Veterinary Sciences (South Australia). For immunoblotting, cell lysates were subjected to SDS-PAGE and transferred to polyvinylidene difluoride (PVDF) microporous membrane filters as described previously (19). Culture supernatants were prepared by filtering (0.22 μm) to remove intact bacterial cells and concentrating 100x by size exclusion centrifugal filtration. Serum raised against the extracellular portion of FdeC was used as primary serum and the secondary antibody was alkaline phosphatase-conjugated anti-rabbit immunoglobulin G (Sigma, Castle Hill, NSW, Australia). 5-bromo-

4-chloro-3-indolylphosphate-nitroblue tetraolium (BCIP/NBT) was used as the substrate in the detection process (Sigma).

Construction of *fdeC* and *hns* mutants. The *fdeC* gene was deleted from *E. coli* N39 using a modification of the λ-Red recombinase gene replacement system (20). The kanamycin resistance cassette was amplified from pKD4 using primers 747 (5′-GTGTAGGCTGGAGCTGCTTC) and 748 (5′-CATATGAATATCCTCCTTAGTTC). Approximately 500 bp regions flanking the *fdeC* gene were amplified using primers 2925 (5′-AGTGTTGCGATGGGTAGTGC) and 2926 (5′-GAAGCAGCTCCAGCCTACACGCAGCGGGTCAGAACTGAAT) for the upstream region and 2927 (5′-GAACTAAGGAGGATATTCATATGTGACCTATGGCGGGTACGAA) and 2928 (5′-TTTGCCGGTACGGTATGCAA) for the downstream region. The kanamycin resistance cassette was inserted between these flanking sequences using three-way PCR and the construct was amplified sufficiently to allow the transformation of N39 with approximately 1 μg of DNA. Mutants were selected by growth on kanamycin and confirmed by DNA sequencing using primers 3025 (5′-CCAGCCAGTTCCTTTCGATGCCT) and 3026 (5′-CCGTGTATACCGCCACCGTGA). The mutant strain was referred to as N39*fdeC*. A modification of the above method was used to inactivate the *hns* gene in N39, by amplifying the kanamycin resistance cassette and 500 bp flanking regions directly from EDL933*hns* (strain MS3832) (21) using primers 2361 (5′-TTGTATGAAGATTGCAAC) and 2364 (5′-TTTATCACAGGATAACCT). Replacement of the *hns* gene with the kanamycin resistance cassette was confirmed by DNA sequencing with primers 1935 (5′-TTGCCTGCTGTTCATGTTCC) and 2449 (5′-GCTGGTTACTCACTCATC). This strain was referred to as N39*hns*. To construct a mutant strain lacking both *fdeC* and *hns*, the kanamycin resistance cassette was first removed from N39*fdeC* using pCP20 as

153 previously described (20) and *hns* was inactivated in this strain using a method identical to that
154 described above.
155
156 **Construction of an *fdeC*::*lacZ* reporter in N39.** The *laclZ* genes were replaced with the
157 chloramphenicol resistance cassette from pKD3 in N39 using the method described above, with the
158 following primers: 3286 (5'-TTTGCCCGGAACAAGACCGC), 3287 (5'-
159 GAAGCAGCTCCAGCCTACACTGCGACATCGTATAGCGTTACTGG), 3288 (5'-
160 GAACTAAGGAGGATATTCATATGTAACCGGGCAGGCCATGTCT), and 3289 (5'-
161 ACAACGCCCAGCCAACACAG). The deletion was confirmed by DNA sequencing using primers 3314 (5'-
162 GGCCTGCATCGCACCACTGT) and 3315 (5'-CCCGCGTACCCTGTTCACCG). This strain was referred to as
163 N39*lacIZ* and used as a negative control in the β-galactosidase assays. Similarly, the *fdeC* gene was
164 then replaced with the *lacZ-zeo* cassette amplified from strain UGB1969 (gift from JM Ghigo) with
165 primers 3290 (5'-ATGACCATGATTACGGATTCACTG) and 3291 (5'-TCAGTCCTGCTCCTCGGCCACGAA).
166 Flanking regions were amplified using primers: 3292 (5'-TCGTTCATGAGAAGCATAACGTA), 3293 (5'-
167 CAGTGAATCCGTAATCATGGTCATTGAGATAATTTCCTGATGAAC), 3294 (5'-
168 TTCGTGGCCGAGGAGCAGGACTGATTTTAAGAATATGAAAGTAACATTCT, and 3295 (5'-
169 AAGACGGATATCTATTTCGTCTC). The *lacZ* fusion and correct replacement of the *fdeC* gene was
170 confirmed by DNA sequencing using the same primers used to confirm the *fdeC* mutant in
171 combination with *lacZ-zeo* cassette-specific screening primers 3312 (5'-TGGTGCCGGACAACACCCTG)
172 and 3313 (5'-GCGGGCCTCTTCGCTATTACGC). The chloramphenicol resistance cassette was removed
173 using pCP20 to facilitate further mutagenesis using this antibiotic selection marker and this reporter
174 strain was referred to as N39*fdeC::lacZ*.
175

Transposon mutagenesis. Random transposon mutants were generated in N39*fdeC::lacZ* using the chloramphenicol cassette from pKD3 (20) with mini-Tn*5* ends introduced by amplifying the cassette using primers 2279 (5'-CTGTCTCTTATACACATCTCACGTCTTGAGCGATTGTGTAGG) and 2280 (5'-CTGTCTCTTATACACATCTGACATGGGAATTAGCCATGGTCC) from *Not*I-digested plasmid. The mini-Tn*5*:Cm PCR product was phosphorylated with T4 polynucleotide kinase (NEB) for 90 min at 37°C followed by inactivation for 20 min at 60°C. The phosphorylated DNA was concentrated to at least 400 ng/uL and transposomes were assembled by incubation with transposase (Epicentre, Madison, Wisconsin, USA) at 37°C for 1 h. Electrocompetent N39*fdeC::lacZ* was transformed with the mini-Tn*5*:Cm transposomes and plated on LB containing chloramphenicol and X-gal and incubated at 37°C overnight (16-18 h). Blue colonies were selected for further analysis and the plates were transferred to 43°C for a further overnight incubation. Those colonies that did not develop a blue color upon incubation at the higher temperature were also selected for further analysis. The location of the transposon insertions were determined using inverse PCR. Genomic DNA was digested with *Taq*α1 (NEB), re-ligated with T4 DNA ligase (NEB) and re-circularized DNA containing the transposon sequence was amplified using primers 2240 (5'-GCCGATCAACGTCTCATTTT) and 4027 (5'-AATAAGATCACTACCGGGCG). DNA sequencing using primer 2240 was used to ascertain the sequence immediately flanking the insertion and the genomic location was determined by using a BLASTn search of the O26:H11 strain 11368 genome sequence.

β-galactosidase assay. Reporter strain *lacZ* activity was assayed using a β-galactosidase assay with ortho-nitrophenyl-β-galactoside (ONPG) as substrate (22). The optical density of the bacterial cultures was measured by diluting 75 µL of culture into 900 µL of LB media and reading at 600 nm in a 1 cm cuvette. A matching 75 µL aliquot of each culture was also lysed with 50 µL chloroform, 25 µL 0.1%

199 SDS and 675 µL Z-buffer (60 mM $Na_2HPO_4.2H_2O$, 40 mM $NaH_2PO_4.2H_2O$, 50 mM β-mercaptoethanol,
200 10 mM KCl, 1 mM $MgSO_4.7H_2O$, pH 7.0). Lysed bacteria were equilibrated to 28°C and 150 µL of ONPG
201 substrate (4 mg/mL) was added to each sample. Reactions were stopped by addition of 375 µL 1 M
202 Na_2CO_3 and the time (T) was recorded. Color development was measured by optical density at
203 420 nm in 1 cm cuvettes. Miller Units were calculated using the following formula: 750 x OD_{420} / T x V
204 x OD_{600} (where V is the volume in mL; 0.075).
205
206 **5'-RACE.** The transcription start site of *fdeC* was determined using the 5' RACE System for Rapid
207 Amplification of cDNA Ends, Version 2.0 (Life Technologies, Carlsbad, CA, USA) following the
208 manufacturer's instructions. Two gene specific primers were used for this assay: GSP1 (4083; 5'-
209 AGGAAATACAGGAGTGGC) and GSP2 (4084; 5'-AACTTTATTACCGGAATGGCCAC).
210
211 **DNA curvature prediction and DNA PAGE analysis.** The *fdeC* promoter region was analyzed *in silico*
212 using Bend.it, a program that enables the prediction of a curvature-propensity plot calculated with
213 DNase I-based parameters (23). The curvature is calculated as a vector sum of dinucleotide
214 geometries (roll, tilt and twist angles) and expressed as degrees per helical turn (10.5°/helical turn =
215 1°/bp). Experimentally tested curved motifs produce curvature values of 5–25°/helical turn, whereas
216 straight motifs give values below 5°/helical turn. The *fdeC* 250 bp promoter region was PCR amplified
217 using primers (4062; 5'-AGGTATCTATTTAATGACTTGCAC) and (4063; 5'-TGAGATAATTTCCTGATCAACG)
218 and its curvature experimentally tested by comparing its electrophoretic mobility with that of a 100
219 bp DNA ladder (NEB) on a 0.5X TBE, 7.5% PAGE gel at 4°C.
220

Electromobility shift assay. Electromobility shift assays were performed essentially as previously described (24). H-NS protein was prepared by amplifying *hns* from N39 using primers 4059 (5'-TACTTCCAATCCAATGCAATGAGCGAAGCACTTAAAATTCTG) and 4060 (5'-TTATCCACTTCCAATGTTATTGCTTGATCAGGAAATCGTC), cloned into the pMCSG7 vector using a ligation-independent method and maintained in *E. coli* DH5α. This plasmid was then transferred to *E. coli* BL21 for expression of the recombinant protein by induction with 1 mM IPTG and purification by Ni-NTA Superflow columns (Qiagen) under native conditions (following the manufacturer's instructions). Protein purity was assessed by SDS-PAGE analysis as previously described (19). The *fdeC* promoter region was amplified using primers 4062 (5'-AGGTATCTATTTAATGACTTGCAC) and 4063 (5'-TGAGATAATTTCCTGATGAACG). A DNA mixture comprising the PCR amplified *fdeC* promoter region and *Taq*I-*Ssp*I-digested pBR322 at an equimolar ratio was incubated at room temperature for 15 minutes with 4 µM of native purified H-NS protein in 30 µL of reaction mixture containing H-NS binding buffer (40 mM HEPES, pH 8, 60 mM potassium glutamate, 8 mM magnesium aspartate, 5 mM dithiothreitol, 10% glycerol, 0.1% octylphenoxypolyethoxyethanol, 0.1 mg/ml BSA). DNA fragments and DNA-protein complexes were resolved by gel electrophoresis (0.5 x TBE, 3% Resolution Plus Agarose Cat.no. 200-0040 (Quantum Scientific); 50 V at 4°C) and visualized after staining with ethidium bromide.

Epithelial cell and extracellular matrix adherence assays. The ability of *E. coli* strains to adhere to HeLa, HEp-2, or primary bovine rectal epithelial cells epithelial cells was tested as previously described (25, 26). Briefly, confluent cell monolayers were infected with *E. coli* strains at a multiplicity of infection (MOI) of 1:10 and incubated for 1 hour. Non-adherent bacteria were removed by 5 washes with PBS, and cell lysates were serially diluted and plated onto LB agar plates to enumerate adherent

244 bacteria. Adherence to extracellular matrix (ECM) proteins was performed as previously described
245 (16, 21, 27).
246
247 **Analysis of biofilm formation.** Biofilm formation on polystyrene surfaces was assessed in 96-well
248 microtiter plates (Iwaki) essentially as previously described (13). Briefly, the pFdeC and pSU2718
249 plasmids were transferred to the Ag43-negative strain MS427 to create MS427(pFdeC) and
250 MS427(pSU2718). These were grown for 24 h in glucose M9 minimal medium (containing 1 mM IPTG
251 for induction of gene expression and 30 μg/mL chloramphenicol) at 28°C or 37°C, washed to remove
252 unbound cells and stained with crystal violet. Quantification of bound cells was assessed by adding
253 acetone–ethanol (20:80) to dissolve the crystal violet, and the optical density was measured at
254 595 nm. To analyse biofilm formation under continuous flow conditions, pFdeC or pSU2718 (vector
255 control) were transferred into *E. coli* OS56, which is identical to MS427 excepting that it constitutively
256 expresses green fluorescent protein (Gfp) to allow analysis by confocal microscopy (12, 13). Flow cells
257 were inoculated with cultures standardized by optical density at 600 nm after overnight growth in
258 glucose M9 minimal medium. OS56(pFdeC) and OS56(pSU2718) biofilms were grown in M9 minimal
259 medium at 28ºC on Rinzl plastic coverslips (ProSciTech, Kirwan, QLD, Australia) in the presence of
260 chloramphenicol and IPTG for maintenance of plasmids and induction of gene expression as described
261 previously (16, 28, 29). Biofilm development was monitored by confocal scanning laser microscopy at
262 24 h or 36 h after inoculation. For analysis of the flow cell biofilms, 14 z-stacks were collected for each
263 strain and analyzed using the COMSTAT software program (30). Comstat data was analyzed using the
264 nonparametric Kruskal-Wallis test within the Minitab (v.14) software package. *P* values < 0.05 were
265 considered significant.

Microscopy and image analysis. Polyclonal FdeC-specific rabbit anti-serum was used for immunofluorescence microscopy (x100 objective) essentially as previously described (28, 31). Immunofluorescence microscopy and image acquisition were performed on a scanning confocal laser microscope (Axioplan2, Zeiss) equipped with detectors and filters for monitoring fluorescein isothiocyanate (FITC) fluorescence. Microscopic observations of biofilms and image acquisition were performed on a scanning confocal laser microscope (LSM510 META, Zeiss, Jena, Thuringia, Germany) equipped with detectors and filters for monitoring of green fluorescent protein (gfp). Vertical cross sections through the biofilms were visualized using the Zeiss LSM Image Examiner. Images were further processed for display by using Photoshop software (Adobe, Mountain View, California, USA).

277 **Results**

278 **Genomic context of *fdeC.*** The genomic context of the *fdeC* gene in non-O157:H7 and O157:H7 EHEC
279 strains was examined using complete and draft genome sequences available on the NCBI database
280 and our own collection. All non-O157:H7 EHEC strains possessed a conserved *fdeC* sequence
281 organisation that is represented by the O26:H11 strains N39 and 11369 (Fig. 1). In contrast, all O157
282 EHEC strains, as represented by the archetypal strain EDL933 possess two additional DNA segments in
283 the region upstream of the *fdeC* gene and downstream of the adjacent *ecp* locus. The sequence
284 between *fdeC* and the *ecp* locus in non-O157:H7 and O157:H7 EHEC strains differs from that
285 previously described for the ExPEC strains CFT073 and IHE3034 (8). Despite these differences, the 550
286 bp region upstream of the *fdeC* coding sequence was conserved in all strains, even in *E. coli* K-12
287 where *fdeC* is truncated to 875 nucleotides (GenBank accession U00096.3, range 314357 to 315232)
288 (32). We hypothesized that this 550 bp region contained the regulatory elements that control the
289 transcription of *fdeC*, and demonstrated this in the series of experiments described below.
290

291 **The *fdeC* promoter is active at high temperature.** In order to investigate the regulation of *fdeC*, a
292 reporter strain was constructed using the O26:H11 strain N39. The *lacI-Z* genes of N39 were initially
293 inactivated to generate the strain N39*lacI-Z*, and this strain was subsequently modified by inserting
294 the *lacZ* gene as a chromosomally-located transcriptional fusion to the *fdeC* promoter to generate the
295 strain N39*lacI-Z fdeC::lacZ-zeo*. When grown on X-gal plates, all N39*lacI-Z fdeC::lacZ-zeo* colonies were
296 white (indicating no transcription). No color heterogeneity was observed among the N39*lacI-Z*
297 *fdeC::lacZ-zeo* colonies at either 37°C or 43°C, indicating that the transcription of *fdeC* is not phase
298 variable. The N39*lacI-Z fdeC::lacZ-zeo* reporter strain was grown under various laboratory culture
299 conditions, including different NaCl concentrations, pH and acetate concentrations, without observing

any difference in β-galactosidase activity (data not shown). However, β-galactosidase activity increased significantly when cells were grown at or above 39°C, compared to 37°C and below (Fig. 2A). This indicated that the *fdeC* promoter is active at temperatures ≥39°C, but repressed at lower temperatures.

FdeC is expressed by wild-type EHEC strains at high temperature. Based on the above transcriptional data, we examined the expression of FdeC in wild-type strains using a FdeC-specific antibody. Western blot analysis of whole cell lysates prepared from N39 revealed strong expression of FdeC at 43°C, a lower level of expression at 39°C, but no expression at 28°C or 37°C (Fig. 2B). A *fdeC* mutant of N39 did not produce FdeC at any of these temperatures, confirming the specificity of the antibody. The same experiment was also performed using the O157:H7 strain EDL933 and the UPEC strain CFT073, and the same temperature-dependent expression of FdeC was observed (Fig. 2B and data not shown). Taken together, the data demonstrate that FdeC expression is temperature regulated and stimulated at or above 39°C. Furthermore, the temperature regulation of *fdeC* in N39, EDL933 and CFT073 is identical, suggesting that the genetic basis of this transcriptional control occurs within the conserved 550 bp DNA region upstream of the *fdeC* open reading frame.

Promoter organization of *fdeC.* The transcription start site for *fdeC* was determined using 5'-RACE and located to a position 184 bp upstream of the *fdeC* ATG translation start site (Fig. 3). The transcription start site is preceded by a strong -10 promoter consensus sequence (5'-TATAAT-3'). A weak -35 promoter consensus sequence (5'-CTAAAT-3') was identified with a 19 bp spacer region. In line with the temperature regulation observed for *fdeC* transcription, bioinformatic analysis revealed the presence of a putative H-NS nucleation site (5'-TGGATATATT-3') (33, 34) located downstream of

323 the *fdeC* -10 promoter sequence. The presence of this nucleation site suggested that H-NS may be
324 responsible for the strong repression of *fdeC* below 37°C. Indeed, genes repressed by H-NS are often
325 regulated in response to changes in temperature; thus this prediction is consistent with our data.
326
327 **Transcription from the *fdeC* promoter is repressed by H-NS.** To test if the transcription of *fdeC* is
328 repressed by H-NS, we mutated the *hns* gene in the N39*lacI-Z fdeC::lacZ-zeo* reporter strain. β-
329 galactosidase activity in the N39*lacI-Z fdeC::lacZ-zeo hns* mutant was significantly increased compared
330 to the parent N39*lacI-Z fdeC::lacZ-zeo* strain following growth at 37ºC (Fig. 4A). Complementation of
331 the N39*lacI-Z fdeC::lacZ-zeo hns* mutant with a *hns*-containing plasmid (pHNS) restored repression,
332 while a vector control strain possessed similarly high β-galactosidase activity to the N39*lacI-Z*
333 *fdeC::lacZ-zeo* strain (Fig. 4A). An independent transposon mutagenesis approach was also utilized to
334 identify regulatory genes that alter β-galactosidase activity in N39*fdeC::lacZ* when grown at 37°C. A
335 library of approximately 20,000 mutants was constructed and screened by color development on agar
336 containing X-gal. The transposon insertion site of those colonies that differed in blue color
337 development in comparison to the parent strain was determined by inverse PCR. In this experiment,
338 only the *hns* gene was identified, further supporting the observation that *fdeC* is repressed by H-NS at
339 37°C.
340
341 **FdeC expression is regulated by H-NS.** To directly examine the effect of H-NS on FdeC expression, the
342 *hns* gene was mutated in N39 and EDL933 to generate the strains N39*hns* and EDL933*hns*. Western
343 blot analysis of whole cell lysates prepared from N39*hns* and EDL933*hns* grown at 37°C revealed
344 strong expression of FdeC. In contrast, no expression of FdeC was observed in either parent strain

345 (Fig. 4B). These results demonstrate that *fdeC* is repressed by H-NS in EHEC at 37°C during growth in
346 LB broth.
347
348 **H-NS binds to the promoter region of *fdeC*.** H-NS binds to intrinsically curved regions of DNA. An *in*
349 *silico* generated curvature-propensity plot calculated with DNase I-based parameters suggested that
350 the promoter region of *fdeC* may assume a curved conformation (Fig. 5A). To test this curvature, we
351 amplified the 250 bp PCR products containing the predicted *fdeC* promoter region and examined it by
352 polyacrylamide gel electrophoresis at 4°C as previously described (35, 36). In line with our prediction,
353 the 250 bp *fdeC* promoter region displayed retarded gel electrophoretic mobility compared to non-
354 curved DNA standards (Fig. 5B). In order to investigate whether H-NS influences *fdeC* transcription by
355 direct binding to the *fdeC* promoter, we performed electrophoretic mobility shift assays as described
356 previously (24, 27). A 250 bp PCR product containing the *fdeC* promoter region was generated and
357 mixed with *Taq*I-*Ssp*I-digested pBR322 DNA (which contains the *bla* promoter that has been
358 previously shown to be bound by H-NS (37)). The DNA was incubated with or without purified H-NS
359 protein and subsequently visualised by gel electrophoresis. The 250 bp *fdeC* promoter region and the
360 fragment containing the *bla*-promoter were both retarded in mobility by the addition of 4 µM H-NS
361 (Fig. 5C). In contrast, the pBR322 fragments not containing the *bla*-promoter did not bind H-NS at this
362 concentration.
363
364 ***fdeC* gene expression is suppressed by acetate and low pH.** The *fdeC* gene is located proximal to the
365 *mat*/*ecp* fimbriae-encoding genes, which in addition to temperature and H-NS are also regulated by
366 pH and acetate (38). To examine if these factors also influence transcription of *fdeC*, we examined the
367 reporter activity of N39*fdeC::lacZ* in response to altered pH and acetate concentration when grown at

368 the permissible temperature of 43°C. Reporter activity was decreased at lower pH and increased at
369 higher pH, while increasing acetate concentration decreased reporter activity (Fig. 6). No difference in
370 growth rate was observed under these conditions (data not shown). Taken together, our data
371 suggests that FdeC expression occurs optimally at pH 8.0 and at low acetate concentrations.

372

373 **FdeC is located at the cell surface.** To examine the cellular location of FdeC, the full-length *fdeC* gene
374 from STEC strain N39 was cloned into the pSU2718 expression vector to generate plasmid pFdeC, and
375 allowing inducible expression of the recombinant FdeC from the lac promoter (17). This plasmid was
376 transferred to the *E. coli* K-12 *flu* deletion strain MS427. This strain does not contain an intact *fdeC*
377 gene, and is unable to mediate the classical cell aggregation and biofilm phenotypes associated with
378 Ag43 expression (15). Expression of the FdeC protein in MS427(pFdeC) was confirmed by western blot
379 (data not shown) and surface exposure of FdeC was confirmed by immunofluorescence microscopy
380 (Fig. 7). Thus, the EHEC *fdeC* gene is functional and encodes a protein located at the cell surface.

381

382 **FdeC mediates biofilm formation.** To assess the functional properties of FdeC, we tested its ability to
383 mediate binding to the extracellular matrix (ECM) protein collagen, and to epithelial cells. In our
384 assays, MS427(pFdeC) did not promote significant adherence to collagen, or to HeLa, HEp-2, or
385 primary bovine rectal epithelial cells (data not shown). Next, we assessed the ability of MS427(pFdeC)
386 to form a biofilm in a static non-treated polystyrene microtitre plate model. MS427(pFdeC) was able
387 to form a strong biofilm at both 28°C and 37°C in comparison to the vector control strain (Fig. 8A).
388 Finally, biofilm formation mediated by FdeC was assessed under dynamic conditions using the
389 continuous-flow chamber model (13, 31). In this assay, OS56(FdeC) produced significantly increased

biofilm growth at both 24 h and 36 h compared to the negative control, OS56(pSU2718), after induction with IPTG (Fig. 8B). Comparative analysis of the biofilm formed by these two strains after 36 h revealed significant differences in the level of bio-volume ($P < 0.001$), substratum coverage ($P < 0.001$), surface area to bio-volume ratio ($P < 0.001$), mean thickness ($P = 0.001$) and biofilm roughness ($P = 0.001$). These results demonstrate that FdeC promotes biofilm formation under continuous flow growth conditions in an overexpressing strain.

Discussion

Bacterial adherence to mammalian cells is a complex process involving a wide range of different adhesins, with the complement of surface proteins and their regulation dramatically influencing the outcome of infection. The adherence of EHEC is attributed mainly to the intimin/Tir system and other LEE-associated adhesins, however some non-O157 EHEC strains are able to cause disease despite lacking the LEE (39). This suggests other adhesins are able to compensate for the lack of intimin, for example the long polar fimbriae (40), although no proteins characterized to date appear to completely explain this phenomenon. The majority of *E. coli* genomes include a gene annotated as *eaeH*, which was first described in a comparison of an ETEC genome (H10407) with a laboratory K-12 strain (41). This gene is truncated in K-12 strains and was computationally predicted to encode an adhesin/invasin in genome-wide studies, based on its predicted structural similarity with intimin and the *Yersinia* invasin. This gene is highly prevalent and well conserved across all pathotypes, and the encoded protein has a similar structure to intimin, with an N-terminal β-barrel domain and C-terminal extracellular domain. This family of proteins with an inverted autotransporter structure has recently been designated as type Ve and shown to be secreted in a similar manner to traditional autotransporters (10). This intimin-like protein was recently characterised in UPEC and named FdeC (8). FdeC was shown to influence adherence of UPEC to bladder epithelial cells and collagen I, III, V, and VI, and enhance virulence in a mouse model of UTI. Here, we have examined the regulation and function of *fdeC* in EHEC.

The previous study in UPEC reported that FdeC is not expressed under laboratory conditions, but is induced when UPEC comes into contact with mammalian cells, and that it can influence the progression of infection in a mouse UTI model (8). Our initial aim was therefore to investigate the

419 mechanism of repression of *fdeC* and determine conditions under which this protein is produced by
420 EHEC. We therefore constructed a *lacZ* reporter strain that could be used to analyse *fdeC* promoter
421 activity. After testing various *in vitro* growth conditions we detected a striking increase in promoter
422 activity during growth at or above 39°C compared to 37°C, and we confirmed that FdeC was
423 expressed by EHEC following growth at ≥39°C.
424
425 EHEC are zoonotic pathogens that colonize the terminal rectum of cattle and other ruminants, where
426 the normal temperature is approximately 39°C (42). It has also been demonstrated that the rectal
427 temperature of cattle can rise to temperatures around 41°C when cattle are exposed to high ambient
428 temperatures (43). This suggests that EHEC may possess specific adaptations to growth at
429 temperatures greater than 37°C. Indeed, heat treatment of O157 EHEC at 48°C has been shown to
430 increase the expression of the virulence associated genes *eae*, *hcpA*, *iha*, *lpfA* and *toxB* (44).
431 Interestingly, we could replicate the same pattern of thermoregulation in not only the O157:H7 strain
432 but also in the UPEC strain CFT073, indicating that the mechanism of regulation is likely conserved.
433
434 Analysis of the genomic context of *fdeC* in a range of *E. coli* pathotypes indicated that there is a
435 conserved 550 bp region immediately upstream of *fdeC* that we hypothesized to be involved in its
436 regulation. The transcription start site of *fdeC* was determined by 5'-RACE to be 184 bp upstream of
437 the predicted ATG start codon and we therefore chose to analyze this sequence in more detail.
438 Bioinformatic analysis detected a putative H-NS nucleation site (33, 34). Additionally, analysis of a
439 random transposon mutant library revealed that a mutation in the *hns* gene led to up-regulation of
440 *fdeC* expression.
441

H-NS is a global regulator involved in the silencing of a number of *E. coli* genes (45, 46). Many *E. coli* H-NS-regulated genes are also thermo-regulated, for example the EIEC *virF* (47), the ETEC heat-labile enterotoxin (LT) (48), the O157:H7 *ehx* operon (49), and the EPEC AIDA-I and its associated glycosyltransferase (50). We therefore sought to confirm whether *fdeC* is repressed by H-NS. Targeted deletion of *hns* in the reporter strain, along with complementation with plasmid-encoded H-NS (pHNS), allowed us to confirm that repression of *fdeC* promoter activity at 37°C is relieved in the absence of H-NS. Construction of *hns* mutants in the EHEC strains N39 and EDL933 confirmed this result at the protein level by western blot. Analysis of a CFT073*hns* mutant also revealed conservation of this regulation in UPEC. A gel shift assay was used to demonstrate direct binding of H-NS proximal to the *fdeC* promoter. Together, this strongly suggests that *fdeC* is directly repressed by H-NS, most likely via its binding to the predicted H-NS nucleation site. However, this alone does not entirely explain the mechanism of *fdeC* regulation.

A predicted RNA thermometer was identified in the 5'-UTR of the *fdeC* transcript. RNA thermometers are regulatory elements that form secondary structures at normal (or lower) temperatures that occlude the ribosome binding site and thereby prevent translation. A rise in temperature destabilizes the RNA secondary structure and allows translation to proceed (51, 52). It would seem likely that in addition to repression of *fdeC* transcription by H-NS, translation of *fdeC* is also directly regulated by temperature via an RNA thermometer. We hypothesize that in the presence of H-NS low-level transcription may be possible, however at low temperatures translation is prevented by the RNA secondary structure. If the temperature increases, then translation is allowed to occur and a low level of protein production is possible. The absence of H-NS results in much higher levels of transcription, however a temperature effect on translation should still occur. Although such a temperature effect is

465 not clear by western blot due to the very high concentration of protein, it was evident in our β-
466 galactosidase assays using the reporter strains (data not shown). In the absence of H-NS, FdeC can be
467 produced at the lower temperature, indicating that repression of translation by the RNA thermometer
468 is not absolute and very high levels of transcript can overcome this regulatory element.
469
470 In the ExPEC strain IHE3034, MatA regulates the *mat* (*ecp*) operon by forming a feedback loop that
471 destabilizes H-NS binding, allowing expression at low temperature, acidic pH and high acetate
472 concentrations (53). As the very highly conserved *mat/ecp* operon is located nearby *fdeC* (Fig. 1) and
473 also regulated by H-NS and temperature, we sought to determine whether pH and acetate
474 concentration would also influence *fdeC* regulation. Analysis of *fdeC* promoter activity under various
475 growth conditions indicated that *fdeC* expression is influenced by pH and acetate concentration
476 inversely to the *mat/ecp* operon, just as it is for altered temperature. That is, assuming the *mat/ecp*
477 operon is regulated similarly in EHEC, while *mat/ecp* is up-regulated by low temperature, low pH and
478 high acetate, *fdeC* is up-regulated by high temperature, high pH and the absence of acetate. Whether
479 or not this apparent inverse relationship is indicative of a linked regulatory mechanism remains to be
480 determined.
481
482 FdeC functions as an adhesin In *E. coli* IHE3034 through its ability to mediate adherence to bladder
483 epithelial cells and collagen (8). We were unable to replicate these results using FdeC cloned from our
484 O26:H11 EHEC strain, with our recombinant *E. coli* MS427(pFdeC) strain failing to adhere to HeLa,
485 Hep2, or primary bovine rectal epithelial cells, nor a range of ECM proteins including collagen. While
486 this may suggest that the cellular adherence function of FdeC is specific to uroepithelial cells, Nesta *et*
487 *al* (8) used a truncated recombinant protein for investigating adherence to ECM proteins while we

488 employed an FdeC over-expression strain, which may account for the discrepancy between the two
489 studies. It is possible that in our system the predicted extracellular domain of FdeC that was
490 demonstrated to mediate attachment by Nesta *et al* (8) is either cleaved from the surface of the
491 recombinant strain, is not folded correctly when over-expressed, or is occluded by other surface
492 proteins. Further study into the function of FdeC in different pathotypes is therefore required. The
493 previous study also demonstrated a role for FdeC in cell aggregation and adherence to glass (8). In this
494 study we examined the role of FdeC in biofilm formation, and demonstrated that its expression in a
495 recombinant K-12 background led to greatly enhanced biofilm formation in both a static plate-based
496 assay and in a continuous flow model.
497
498 In summary, we have characterized the regulation of the intimin-like protein FdeC in EHEC, and
499 identified H-NS as a repressor of *fdeC* transcription. We also show that the expression of FdeC is
500 exquisitely controlled by temperature. FdeC mediates biofilm formation following over-expression in
501 a recombinant strain background, and its expression at ≥39°C suggests it may have a role in EHEC
502 when residing in the terminal rectum of cattle where such temperatures are not abnormal. Future
503 studies will seek to test this hypothesis.
504

505 **Acknowledgements**

506 This work was supported by grants from the Queensland Government Smart Futures National and
507 International Research Alliances Program (2008004328) and the Australian Research Council
508 (DP1097032). MAS is supported by an ARC Future Fellowship (FT100100662). The authors thank
509 researchers from CSIRO Animal, Food and Health Sciences Division for provision of STEC isolates.

References

1. **Karch H, Tarr PI, Bielaszewska M.** 2005. Enterohaemorrhagic *Escherichia coli* in human medicine. Int. J. Med. Microbiol. **295:**405-418.
2. **Nataro JP, Kaper JB.** 1998. Diarrheagenic *Escherichia coli*. Clin. Microbiol. Rev. **11:**142-201.
3. **Gyles CL.** 2007. Shiga toxin-producing *Escherichia coli*: an overview. J. Anim. Sci. **85:**E45-62.
4. **Matthews L, Low JC, Gally DL, Pearce MC, Mellor DJ, Heesterbeek JA, Chase-Topping M, Naylor SW, Shaw DJ, Reid SW, Gunn GJ, Woolhouse ME.** 2006. Heterogeneous shedding of *Escherichia coli* O157 in cattle and its implications for control. Proc. Natl. Acad. Sci. U.S.A. **103:**547-552.
5. **Smith JL, Fratamico PM, Gunther NWt.** 2014. Shiga toxin-producing *Escherichia coli*. Adv. Appl. Microbiol. **86:**145-197.
6. **Bardiau M, Szalo M, Mainil JG.** 2010. Initial adherence of EPEC, EHEC and VTEC to host cells. Vet. Res. **41:**57.
7. **Potter AA, Klashinsky S, Li Y, Frey E, Townsend H, Rogan D, Erickson G, Hinkley S, Klopfenstein T, Moxley RA, Smith DR, Finlay BB.** 2004. Decreased shedding of *Escherichia coli* O157:H7 by cattle following vaccination with type III secreted proteins. Vaccine **22:**362-369.
8. **Nesta B, Spraggon G, Alteri C, Moriel DG, Rosini R, Veggi D, Smith S, Bertoldi I, Pastorello I, Ferlenghi I, Fontana MR, Frankel G, Mobley HL, Rappuoli R, Pizza M, Serino L, Soriani M.** 2012. FdeC, a novel broadly conserved *Escherichia coli* adhesin eliciting protection against urinary tract infections. MBio. **3**.

9. **Moriel DG, Bertoldi I, Spagnuolo A, Marchi S, Rosini R, Nesta B, Pastorello I, Corea VA, Torricelli G, Cartocci E, Savino S, Scarselli M, Dobrindt U, Hacker J, Tettelin H, Tallon LJ, Sullivan S, Wieler LH, Ewers C, Pickard D, Dougan G, Fontana MR, Rappuoli R, Pizza M, Serino L.** 2010. Identification of protective and broadly conserved vaccine antigens from the genome of extraintestinal pathogenic *Escherichia coli*. Proc. Natl. Acad. Sci. U.S.A. **107:**9072-9077.

10. **Oberhettinger P, Schütz M, Leo JC, Heinz N, Berger J, Autenrieth IB, Linke D.** 2012. Intimin and invasin export their C-terminus to the bacterial cell surface using an inverse mechanism compared to classical autotransport. PLoS One **7:**e47069.

11. **Atlung T, Ingmer H.** 1997. H-NS: a modulator of environmentally regulated gene expression. Mol. Microbiol. **24:**7-17.

12. **Perna NT, Plunkett G, 3rd, Burland V, Mau B, Glasner JD, Rose DJ, Mayhew GF, Evans PS, Gregor J, Kirkpatrick HA, Pósfai G, Hackett J, Klink S, Boutin A, Shao Y, Miller L, Grotbeck EJ, Davis NW, Lim A, Dimalanta ET, Potamousis KD, Apodaca J, Anantharaman TS, Lin J, Yen G, Schwartz DC, Welch RA, Blattner FR.** 2001. Genome sequence of enterohaemorrhagic *Escherichia coli* O157:H7. Nature **409:**529-533.

13. **Kjaergaard K, Schembri MA, Ramos C, Molin S, Klemm P.** 2000. Antigen 43 facilitates formation of multispecies biofilms. Environ. Microbiol. **2:**695-702.

14. **Sherlock O, Schembri MA, Reisner A, Klemm P.** 2004. Novel roles for the AIDA adhesin from diarrheagenic *Escherichia coli*: cell aggregation and biofilm formation. J. Bacteriol. **186:**8058-8065.

15. **Reisner A, Haagensen JA, Schembri MA, Zechner EL, Molin S.** 2003. Development and maturation of *Escherichia coli* K-12 biofilms. Mol. Microbiol. **48:**933-946.

16. **Allsopp LP, Beloin C, Ulett GC, Valle J, Totsika M, Sherlock O, Ghigo JM, Schembri MA.** 2012. Molecular characterization of UpaB and UpaC, two new autotransporter proteins of uropathogenic *Escherichia coli* CFT073. Infect. Immun. **80:**321-332.

17. **Martinez E, Bartolomé B, de la Cruz F.** 1988. pACYC184-derived cloning vectors containing the multiple cloning site and lacZ alpha reporter gene of pUC8/9 and pUC18/19 plasmids. Gene **68:**159-162.

18. **Donnelly MI, Zhou M, Millard CS, Clancy S, Stols L, Eschenfeldt WH, Collart FR, Joachimiak A.** 2006. An expression vector tailored for large-scale, high-throughput purification of recombinant proteins. Protein Expr. Purif. **47:**446-454.

19. **Ulett GC, Webb RI, Schembri MA.** 2006. Antigen-43-mediated autoaggregation impairs motility in *Escherichia coli*. Microbiology **152:**2101-2110.

20. **Datsenko KA, Wanner BL.** 2000. One-step inactivation of chromosomal genes in *Escherichia coli* K-12 using PCR products. Proc. Natl. Acad. Sci. U.S.A. **97:**6640-6645.

21. **Totsika M, Wells TJ, Beloin C, Valle J, Allsopp LP, King NP, Ghigo J-M, Schembri MA.** 2012. Molecular Characterization of the EhaG and UpaG Trimeric Autotransporter Proteins from Pathogenic *Escherichia coli*. Appl. Environ. Microbiol. **78:**2179-2189.

22. **Miller JH.** 1992. A short course in bacterial genetics: a laboratory manual and handbook for *Escherichia coli* and related bacteria, vol. 1. Cold Spring Harbor Laboratory Pr.

23. **Vlahovicek K, Kajan L, Pongor S.** 2003. DNA analysis servers: plot.it, bend.it, model.it and IS. Nucleic Acids Res. **31:**3686-3687.

24. **Beloin C, Dorman CJ.** 2003. An extended role for the nucleoid structuring protein H-NS in the virulence gene regulatory cascade of *Shigella flexneri*. Mol. Microbiol. **47:**825-838.

25. **Wells TJ, Sherlock O, Rivas L, Mahajan A, Beatson SA, Torpdahl M, Webb RI, Allsopp LP, Gobius KS, Gally DL, Schembri MA.** 2008. EhaA is a novel autotransporter protein of

enterohemorrhagic *Escherichia coli* O157:H7 that contributes to adhesion and biofilm formation. Environ. Microbiol. **10:**589-604.

26. **Mabbett AN, Ulett GC, Watts RE, Tree JJ, Totsika M, Ong CL, Wood JM, Monaghan W, Looke DF, Nimmo GR, Svanborg C, Schembri MA.** 2009. Virulence properties of asymptomatic bacteriuria *Escherichia coli*. Int. J. Med. Microbiol. **299:**53-63.

27. **Allsopp LP, Beloin C, Moriel DG, Totsika M, Ghigo JM, Schembri MA.** 2012. Functional Heterogeneity of the UpaH Autotransporter Protein from Uropathogenic Escherichia coli. J. Bacteriol. **194:**5769-5782.

28. **Valle J, Mabbett AN, Ulett GC, Toledo-Arana A, Wecker K, Totsika M, Schembri MA, Ghigo JM, Beloin C.** 2008. UpaG, a new member of the trimeric autotransporter family of adhesins in uropathogenic *Escherichia coli*. J. Bacteriol. **190:**4147-4161.

29. **Ulett GC, Valle J, Beloin C, Sherlock O, Ghigo JM, Schembri MA.** 2007. Functional analysis of antigen 43 in uropathogenic *Escherichia coli* reveals a role in long-term persistence in the urinary tract. Infect. Immun. **75:**3233-3244.

30. **Heydorn A, Nielsen AT, Hentzer M, Sternberg C, Givskov M, Ersboll BK, Molin S.** 2000. Quantification of biofilm structures by the novel computer program COMSTAT. Microbiology **146:**2395-2407.

31. **Allsopp LP, Totsika M, Tree JJ, Ulett GC, Mabbett AN, Wells TJ, Kobe B, Beatson SA, Schembri MA.** 2010. UpaH is a newly identified autotransporter protein that contributes to biofilm formation and bladder colonization by uropathogenic *Escherichia coli* CFT073. Infect. Immun. **78:**1659-1669.

32. **Blattner FR, Plunkett G, 3rd, Bloch CA, Perna NT, Burland V, Riley M, Collado-Vides J, Glasner JD, Rode CK, Mayhew GF, Gregor J, Davis NW, Kirkpatrick HA, Goeden MA,**

Rose DJ, Mau B, Shao Y. 1997. The complete genome sequence of *Escherichia coli* K-12. Science **277:**1453-1462.

33. **Bouffartigues E, Buckle M, Badaut C, Travers A, Rimsky S.** 2007. H-NS cooperative binding to high-affinity sites in a regulatory element results in transcriptional silencing. Nat Struct Mol Biol **14:**441-448.

34. **Lang B, Blot N, Bouffartigues E, Buckle M, Geertz M, Gualerzi CO, Mavathur R, Muskhelishvili G, Pon CL, Rimsky S, Stella S, Babu MM, Travers A.** 2007. High-affinity DNA binding sites for H-NS provide a molecular basis for selective silencing within proteobacterial genomes. Nucleic Acids Res **35:**6330-6337.

35. **Ussery DW, Higgins CF, Bolshoy A.** 1999. Environmental influences on DNA curvature. J. Biomol. Struct. Dyn. **16:**811-823.

36. **Yamada H, Muramatsu S, Mizuno T.** 1990. An *Escherichia coli* protein that preferentially binds to sharply curved DNA. J. Biochem. **108:**420-425.

37. **Zuber F, Kotlarz D, Rimsky S, Buc H.** 1994. Modulated expression of promoters containing upstream curved DNA sequences by the *Escherichia coli* nucleoid protein H-NS. Mol. Microbiol. **12:**231-240.

38. **Lehti TA, Bauchart P, Kukkonen M, Dobrindt U, Korhonen TK, Westerlund-Wikstrom B.** 2013. Phylogenetic group-associated differences in regulation of the common colonization factor Mat fimbria in *Escherichia coli*. Mol. Microbiol. **87:**1200-1222.

39. **Newton HJ, Sloan J, Bulach DM, Seemann T, Allison CC, Tauschek M, Robins-Browne RM, Paton JC, Whittam TS, Paton AW, Hartland EL.** 2009. Shiga toxin-producing *Escherichia coli* strains negative for locus of enterocyte effacement. Emerg. Infect. Dis. **15:**372-380.

40. **Galli L, Torres AG, Rivas M.** 2010. Identification of the long polar fimbriae gene variants in the locus of enterocyte effacement-negative Shiga toxin-producing *Escherichia coli* strains isolated from humans and cattle in Argentina. FEMS Microbiol. Lett. **308:**123-129.

41. **Chen Q, Savarino SJ, Venkatesan MM.** 2006. Subtractive hybridization and optical mapping of the enterotoxigenic *Escherichia coli* H10407 chromosome: isolation of unique sequences and demonstration of significant similarity to the chromosome of *E. coli* K-12. Microbiology **152:**1041-1054.

42. **Reid ED, Fried K, Velasco JM, Dahl GE.** 2012. Correlation of rectal temperature and peripheral temperature from implantable radio-frequency microchips in Holstein steers challenged with lipopolysaccharide under thermoneutral and high ambient temperatures. J. Anim. Sci.

43. **Gaughan JB, Bonner S, Loxton I, Mader TL, Lisle A, Lawrence R.** 2010. Effect of shade on body temperature and performance of feedlot steers. J. Anim. Sci. **88:**4056-4067.

44. **Slanec T, Schmidt H.** 2011. Specific expression of adherence-related genes in *Escherichia coli* O157:H7 strain EDL933 after heat treatment in ground beef. J. Food. Prot. **74:**1434-1440.

45. **Dorman CJ.** 2013. Co-operative roles for DNA supercoiling and nucleoid-associated proteins in the regulation of bacterial transcription. Biochem. Soc. Trans. **41:**542-547.

46. **Fang FC, Rimsky S.** 2008. New insights into transcriptional regulation by H-NS. Curr. Opin. Microbiol. **11:**113-120.

47. **Colonna B, Casalino M, Fradiani PA, Zagaglia C, Naitza S, Leoni L, Prosseda G, Coppo A, Ghelardini P, Nicoletti M.** 1995. H-NS regulation of virulence gene expression in enteroinvasive *Escherichia coli* harboring the virulence plasmid integrated into the host chromosome. J. Bacteriol. **177:**4703-4712.

48. **Trachman JD, Yasmin M.** 2004. Thermo-osmoregulation of heat-labile enterotoxin expression by *Escherichia coli*. Curr. Microbiol. **49:**353-360.

49. **Li H, Granat A, Stewart V, Gillespie JR.** 2008. RpoS, H-NS, and DsrA influence EHEC hemolysin operon (ehxCABD) transcription in *Escherichia coli* O157:H7 strain EDL933. FEMS Microbiol. Lett. **285:**257-262.

50. **Benz I, van Alen T, Bolte J, Wormann ME, Schmidt MA.** 2010. Modulation of transcription and characterization of the promoter organization of the autotransporter adhesin heptosyltransferase and the autotransporter adhesin AIDA-I. Microbiology **156:**1155-1166.

51. **Chowdhury S, Maris C, Allain FH, Narberhaus F.** 2006. Molecular basis for temperature sensing by an RNA thermometer. EMBO J. **25:**2487-2497.

52. **Narberhaus F, Waldminghaus T, Chowdhury S.** 2006. RNA thermometers. FEMS Microbiol. Rev. **30:**3-16.

53. **Lehti TA, Heikkinen J, Korhonen TK, Westerlund-Wikström B.** 2012. The response regulator RcsB activates expression of Mat fimbriae in meningitic *Escherichia coli*. J. Bacteriol. **194:**3475-3485.

54. **Sullivan MJ, Petty NK, Beatson SA.** 2011. Easyfig: a genome comparison visualizer. Bioinformatics **27:**1009-1010.

671 **Figure legends**

672

673 **Figure 1. The genomic context of *fdeC.*** The genomic context of *fdeC* (red) is shown in the O26:H11
674 STEC strains (N39 and 11368) and other pathogenic *E. coli* strains (O157:H7 STEC strain EDL933 and
675 UPEC strain CFT073). Variable regions (green) between *fdeC* and the *mat/ecp* operon (blue) are
676 illustrated. The genomic comparison was performed using Easyfig (54); The grey shading indicates
677 high nucleotide identity between the sequences (95-100%).

678

679 **Figure 2. Temperature-dependent expression of FdeC. (A)** β-galactosidase activity (in Miller Units)
680 from N39*lacIZ* (control) and N39*fdeC::lacIZ* grown at various temperatures. The *fdeC* promoter was
681 only active at 39°C and 43°C **(B)** Western blot analysis of STEC strains N39, N39*fdeC* and EDL933
682 grown at 28°C, 37°C, 39°C and 43°C. Similar to the reporter assay, FdeC expression was only detected
683 at or above 39°C.

684

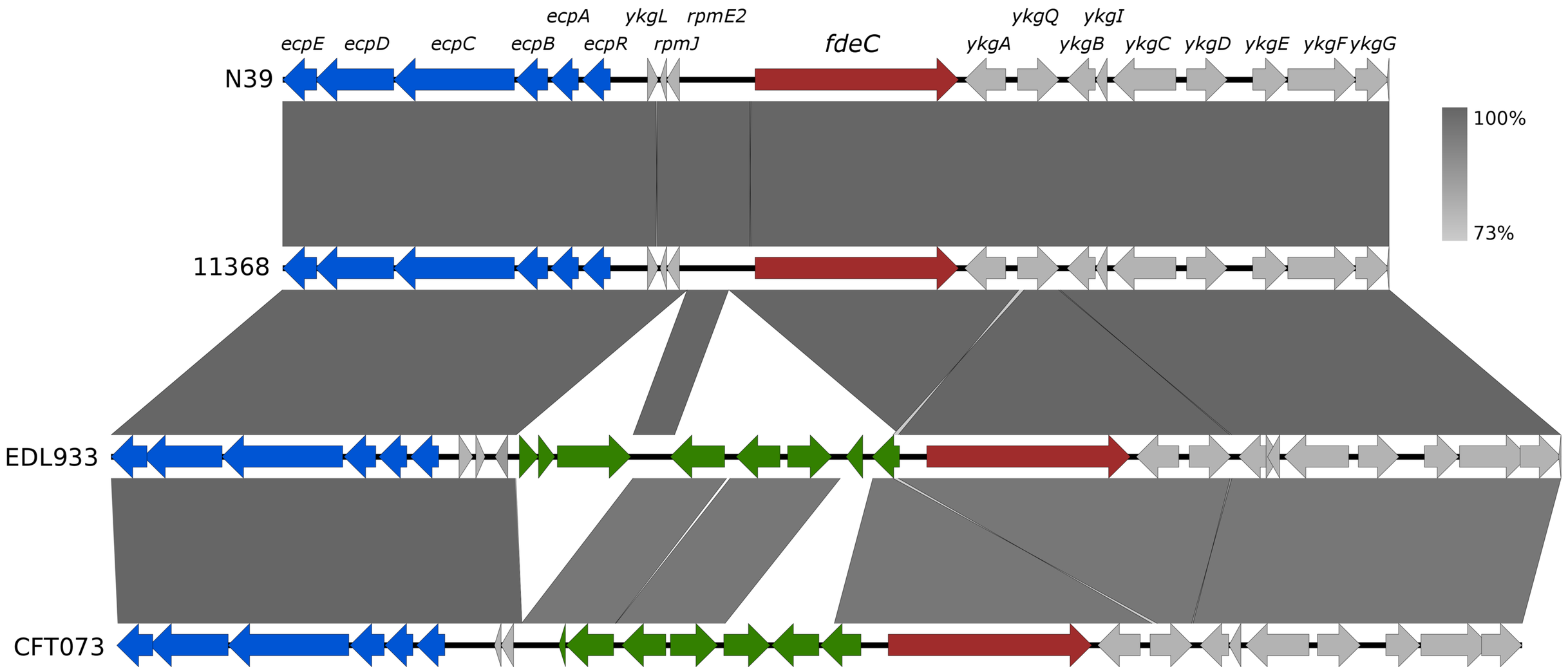
685 **Figure 3. Promoter organization of the *fdeC* gene.** Structural organization of the *fdeC* promoter
686 indicating the -10 and -35 elements, transcription start site (arrowhead), ribosome binding site (RBS)
687 and ATG start codon. Also indicated is a putative H-NS nucleation site (bold and over-lined). The
688 primer binding sites for the region amplified for use in the electromobility shift assay are indicated by
689 arrows below the sequence.

690

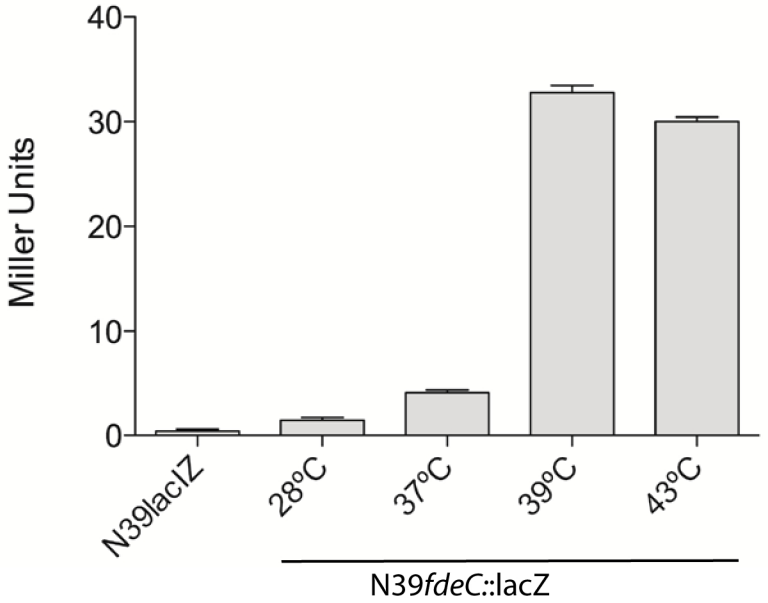
691 **Figure 4. Repression of *fdeC* transcription by H-NS. (A)** β-galactosidase activity (in Miller Units) from
692 N39*lacIZ* (control), N39*fdeC::lacIZ*, N39*fdeC::lacIZ hns*, N39*fdeC::lacIZ hns* (pHNS) and N39*fdeC::lacIZ*
693 *hns* (pBR322). Mutation of the *hns* gene (N39*fdeC::lacIZ hns*) resulted in an increase in β-galactosidase

694 activity, which could be reduced by complementation with *hns* on a plasmid (N39*fdeC::lacIZ hns*
695 [pHNS]). **(B)** Western blot analysis of FdeC performed using whole-cell lysates prepared from N39
696 (WT), N39*fdeC*, N39*hns*, N39*fdeC hns*, EDL933 (WT) and EDL933*hns*. The band representing the
697 predicted FdeC extracellular domain (~100 kDa) is indicated. The higher molecular weight cross-
698 reacting band likely represents the full length FdeC protein.
699
700 **Figure 5. H-NS binds to the promoter region of *fdeC.* (A)** *In silico* curvature-propensity plot showing
701 predicted regions of curved DNA in the 250 bp PCR fragment containing the *fdeC* promoter. **(B)**
702 Electrophoretic mobility of the 250 bp PCR fragment containing the *fdeC* promoter. Migration of this
703 band is slightly retarded in the gel suggesting that the DNA is curved. **(C)** Electrophoretic band shift of
704 the 250 bp PCR fragment containing the *fdeC* promoter and the *bla* promoter from *Taq*I-*Ssp*I digested
705 pBR322 DNA in the absence or presence of 4 µM H-NS. The migration of pBR322 fragments not
706 containing the *bla*-promoter was not altered by H-NS. The image depicts a representative gel of three
707 independent experiments**.**
708
709 **Figure 6. Influence of pH and acetate in *fdeC* promoter activity.** β-galactosidase activity (in Miller
710 Units) from N39*fdeC::lacIZ* grown in the presence of **(A)** increasing concentrations of acetate and **(B)**
711 increasing pH. The *fdeC* promoter was most active in the absence of acetate and at pH 8.0.
712
713 **Figure 7. FdeC is localized at the cell surface.** Immunofluorescence microscopy of the vector control
714 MS427(pSU2718) and complemented strain MS427pFdeC. Phase-contrast (top panel) or
715 immunofluorescence (lower panel) microscopy employing FdeC-specific antiserum against cells of *E.*
716 *coli* strains **(A)** MS427(pSU2718) and **(B)** MS427(pFdeC). Strains were grown in the presence of 1mM

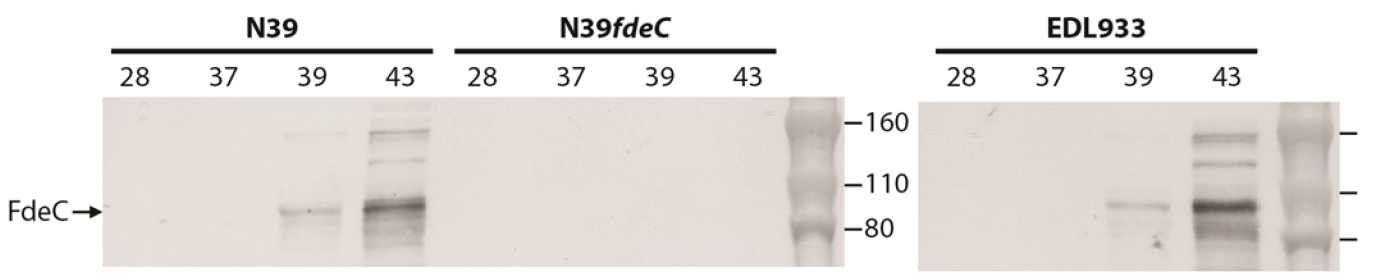
717 IPTG, fixed and incubated with anti-FdeC serum followed by incubation with goat anti-rabbit IgG
718 coupled to Alexa Fluor 488. A positive reaction indicating surface localization of FdeC was detected for
719 MS427(pFdeC).
720
721 **Figure 8. FdeC mediates biofilm formation. (A)** Biofilm formation in polystyrene microtitre plates by
722 the vector control MS427(pSU2718) and MS427(pFdeC) at 28°C and 37°C. Results represent averages
723 of OD_{595} readings of at least 4 independent experiments ± SEM. The expression of FdeC resulted in
724 strong biofilm formation at both temperatures. **(B)** Dynamic flow chamber assay examining biofilm
725 formation of *E. coli* OS56 containing pFdeC (left panel) and the control plasmid pSU2718 (right panel).
726 Biofilm development was monitored by confocal scanning laser microscopy after 36 hours. The
727 images are representative horizontal sections collected within each biofilm and vertical sections (the
728 right and above each larger panel, representing the yz plane and the xz plane, respectively). The
729 expression of FdeC resulted in strong biofilm formation.
730

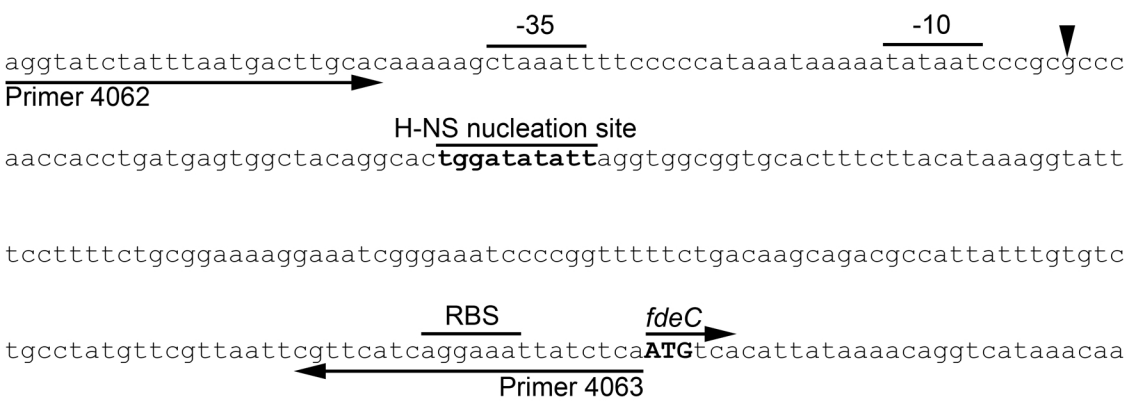

ecpA
ykgL
rpmE2
ykgQ
ykgI
ecpE
ecpD
ecpC
ecpB
ecpR
rpmJ
fdeC
ykgA
ykgB
ykgC
ykgD
ykgE
ykgF
ykgG
N39
11368
EDL933
CFT073
100%
73%

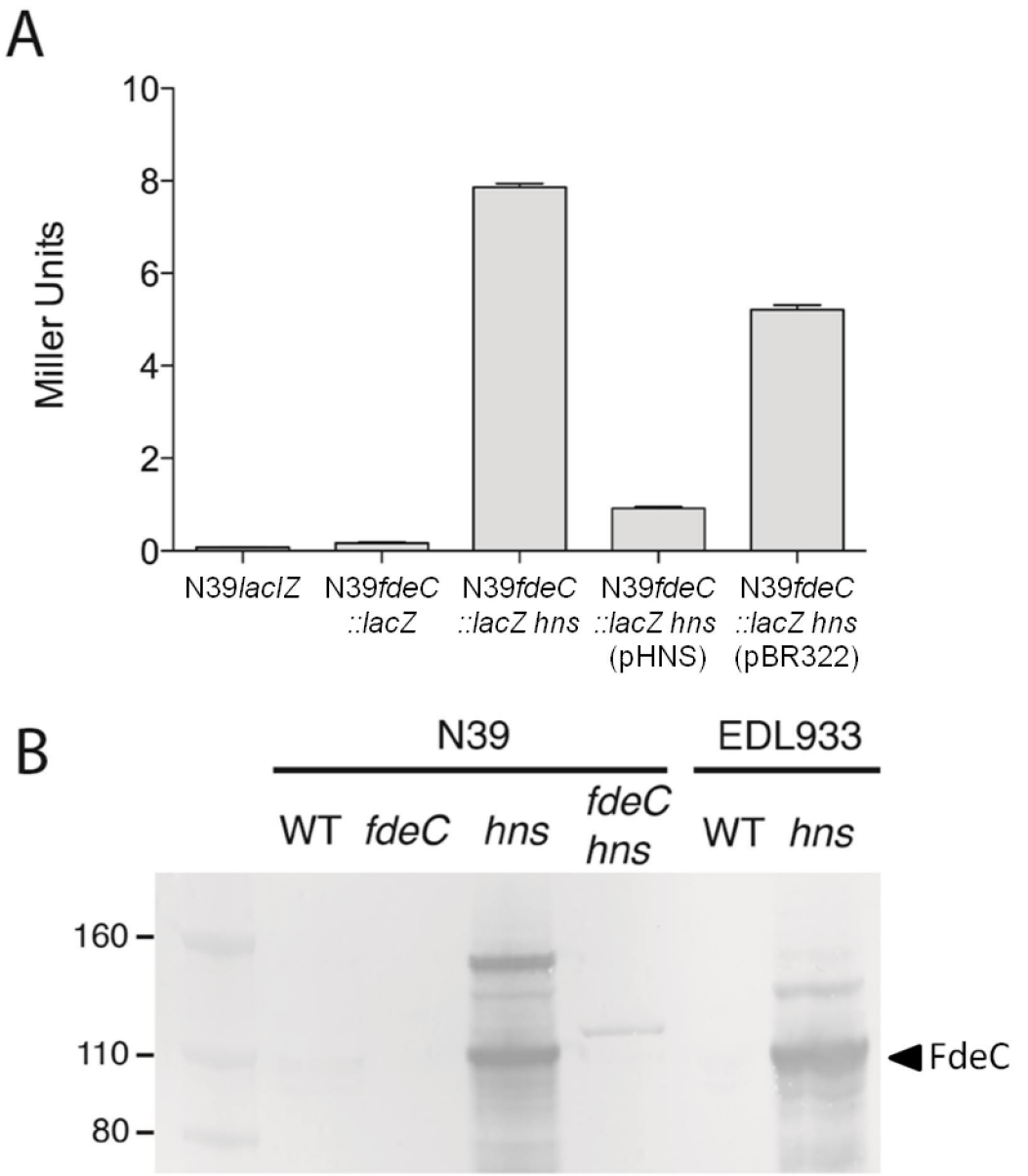
A

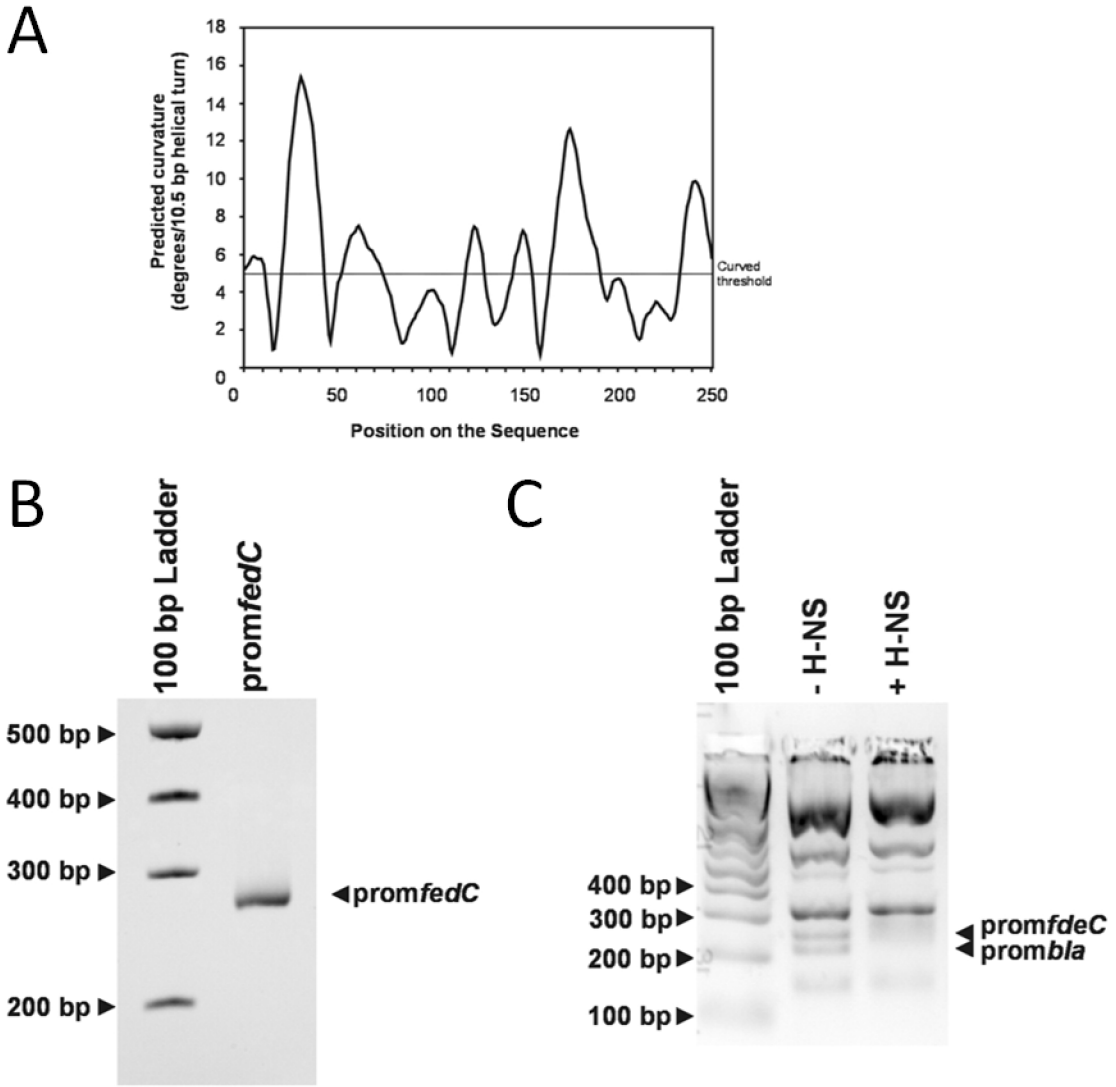

40
30
20
10
0
Miller Units
N39lacIZ
28°C
37°C
39°C
43°C
N39fdeC::lacZ

B

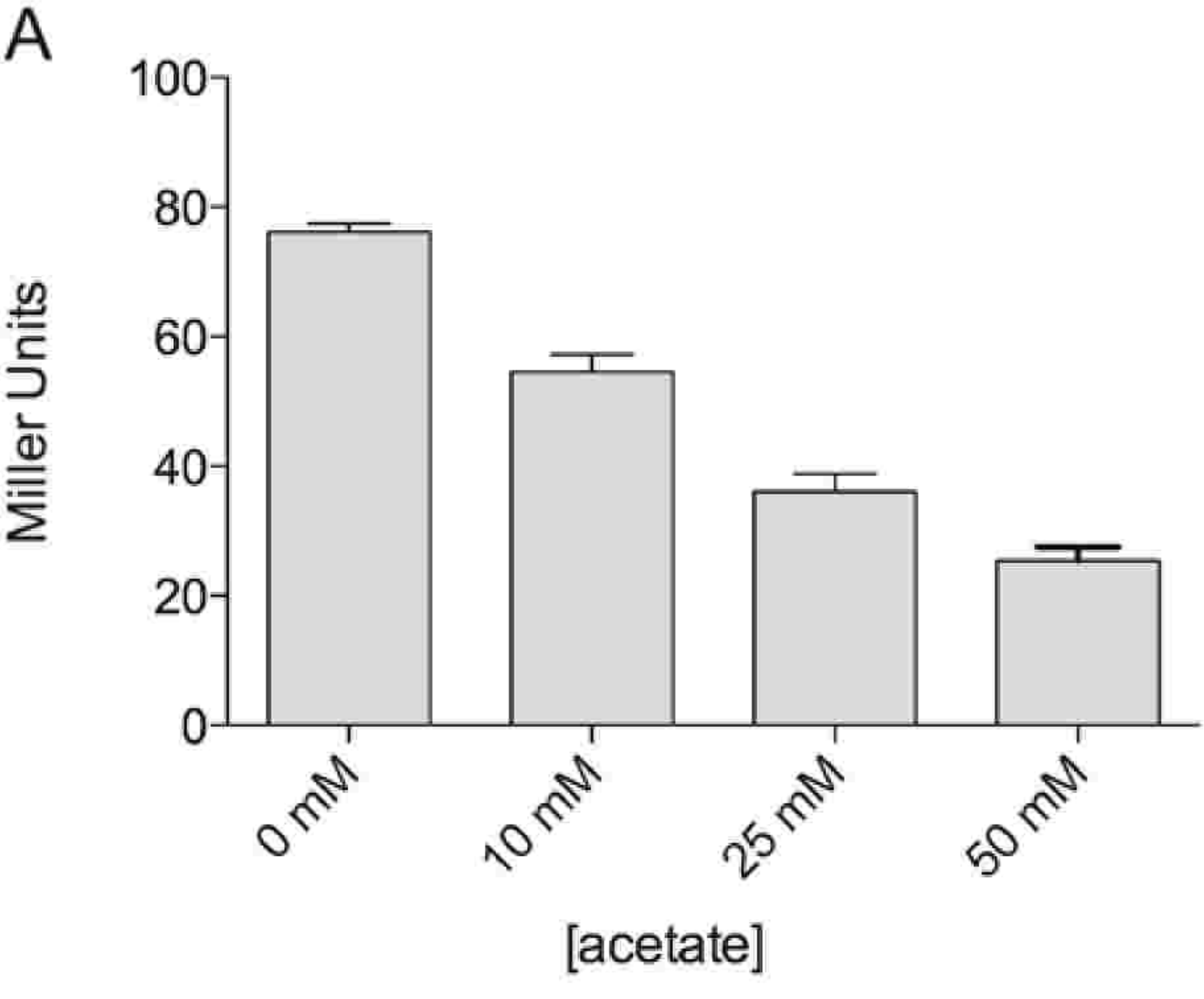

N39
N39fdeC
EDL933
28
37
39
43
28
37
39
43
28
37
39
43
FdeC
160
110
80


-35
-10
aggtatctatttaatgacttgcacaaaaagctaaattttcccccataaataaaaatataatcccgcgccc
Primer 4062
H-NS nucleation site
aaccacctgatgagtggctacaggcactggatatattaggtggcggtgcactttcttacataaaggtatt
tccttttctgcggaaaaggaaatcgggaaatccccggtttttctgacaagcagacgccattatttgtgtc
RBS
fdeC
tgcctatgttcgttaattcgttcatcaggaaattatctcaATGtcacattataaaacaggtcataaacaa
Primer 4063

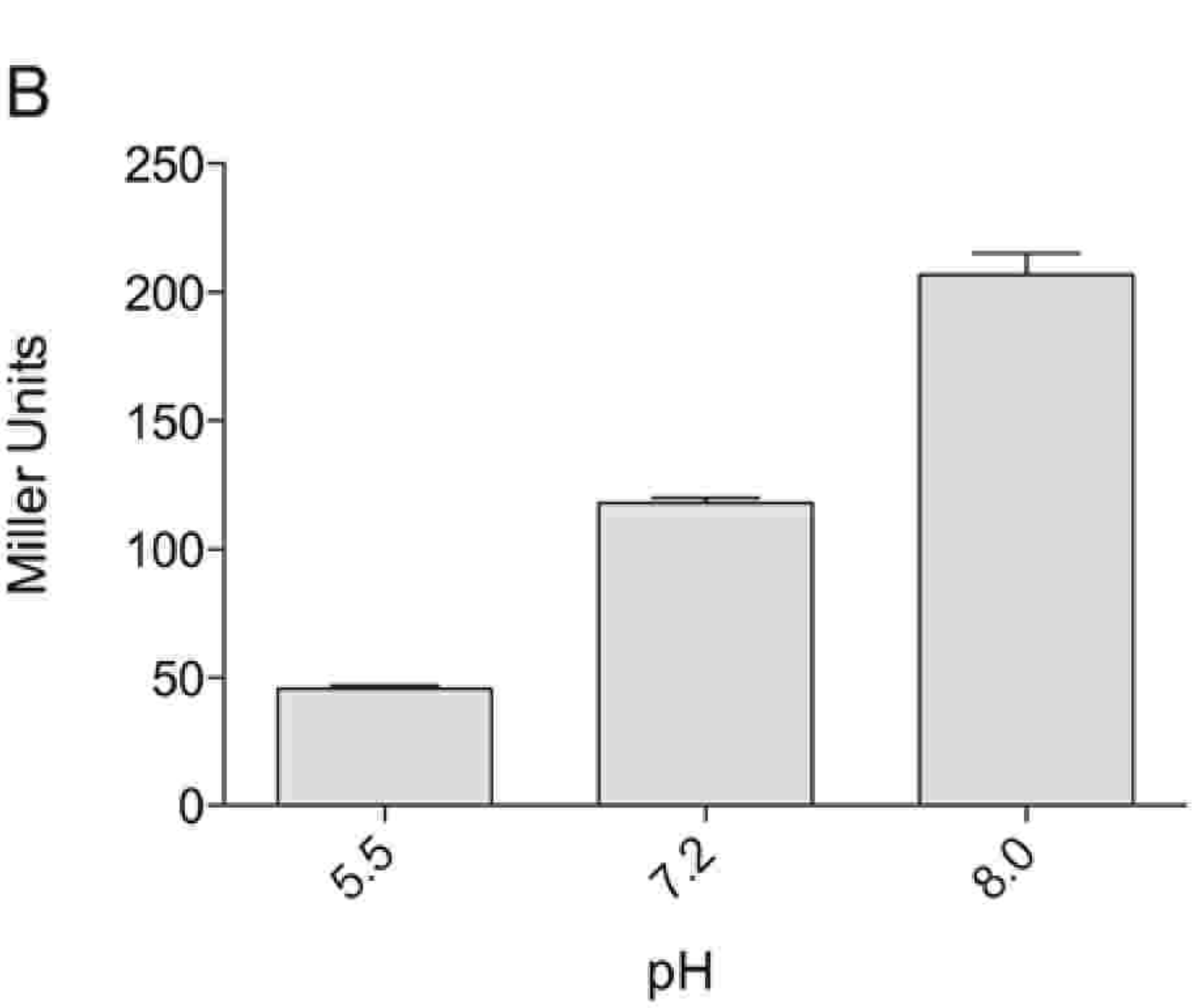

A
Miller Units
10
8
6
4
2
0
N39lacIZ
N39fdeC ::lacZ
N39fdeC ::lacZ hns
N39fdeC ::lacZ hns (pHNS)
N39fdeC ::lacZ hns (pBR322)
B
N39
EDL933
WT
fdeC
hns
fdeC hns
WT
hns
160
110
80
FdeC


A
Predicted curvature
(degrees/10.5 bp helical turn)
18
16
14
12
10
8
6
4
2
0
0
50
100
150
200
250
Position on the Sequence
Curved
threshold
B
100 bp Ladder
prom*fedC*
500 bp
400 bp
300 bp
200 bp
prom*fedC*
C
100 bp Ladder
- H-NS
+ H-NS
400 bp
300 bp
200 bp
100 bp
prom*fdeC*
prom*bla*

A

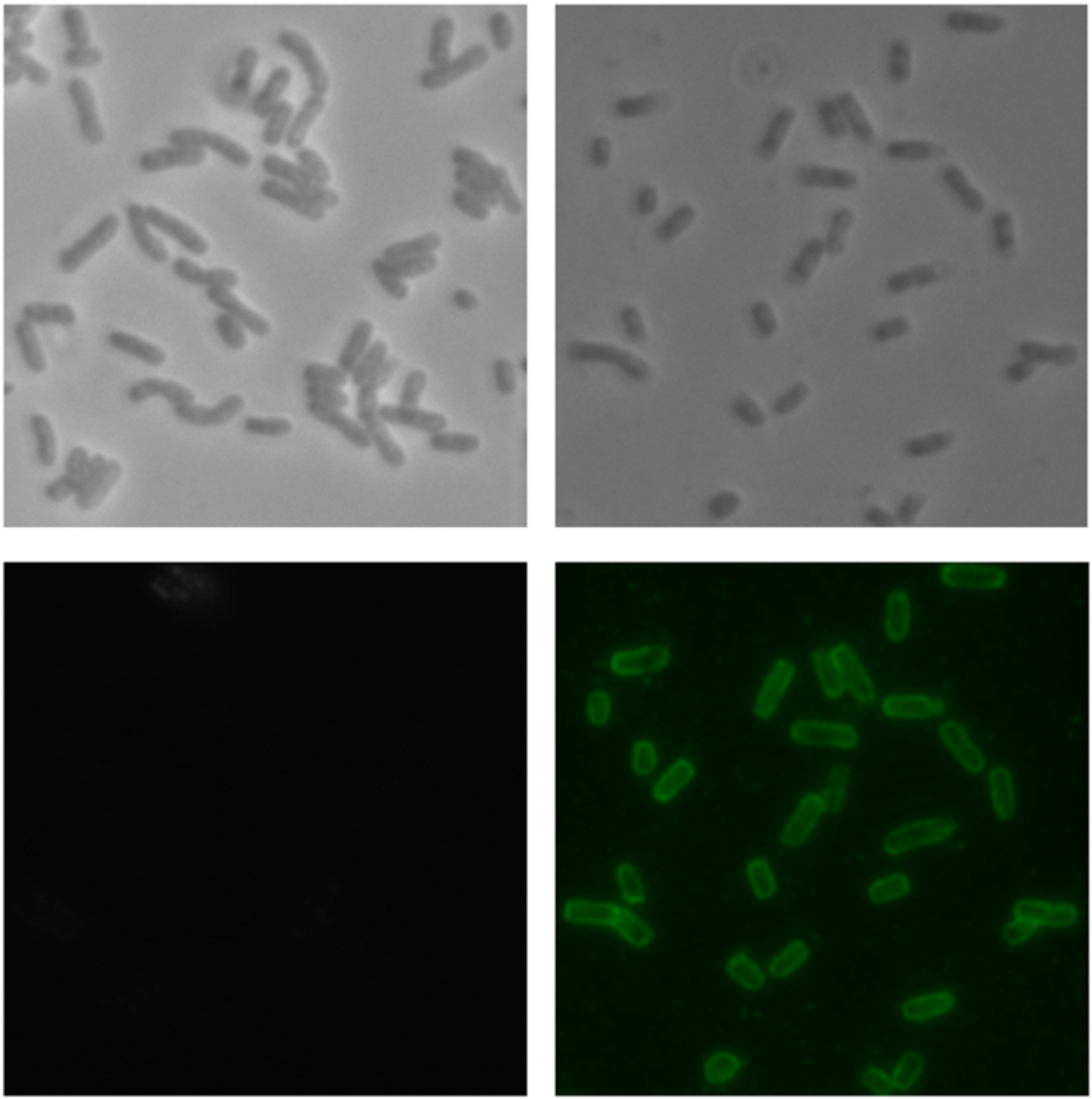

Miller Units
100
80
60
40
20
0
0 mM
10 mM
25 mM
50 mM
[acetate]

B

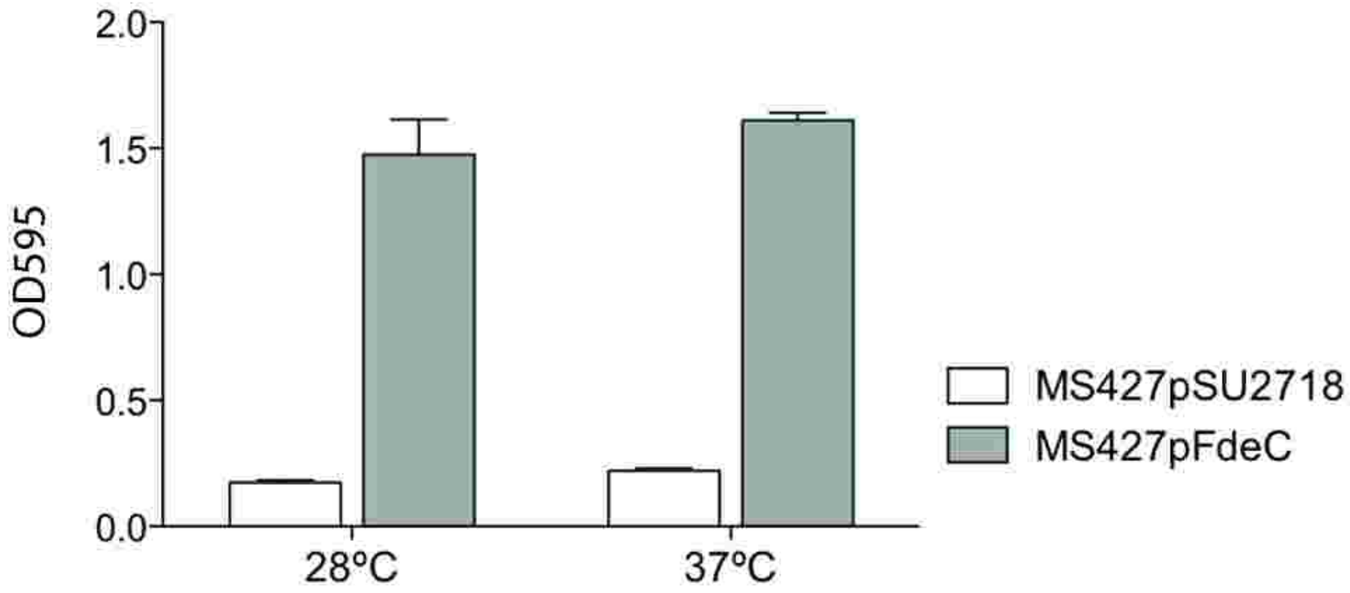

Miller Units
250
200
150
100
50
0
5.5
7.2
8.0
pH

(a) MS427[pSU2718]

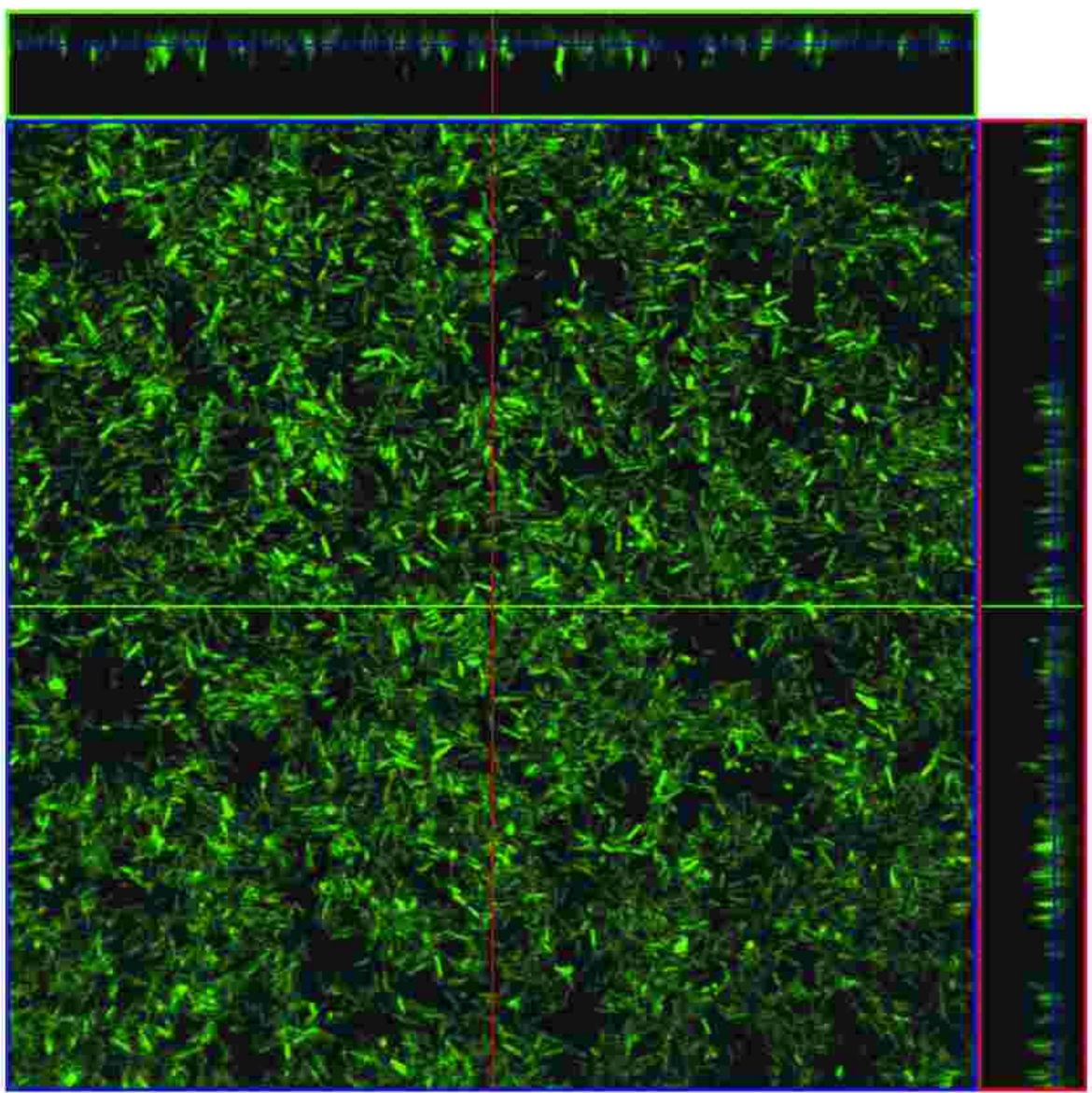
(b) MS427[pFdeC]

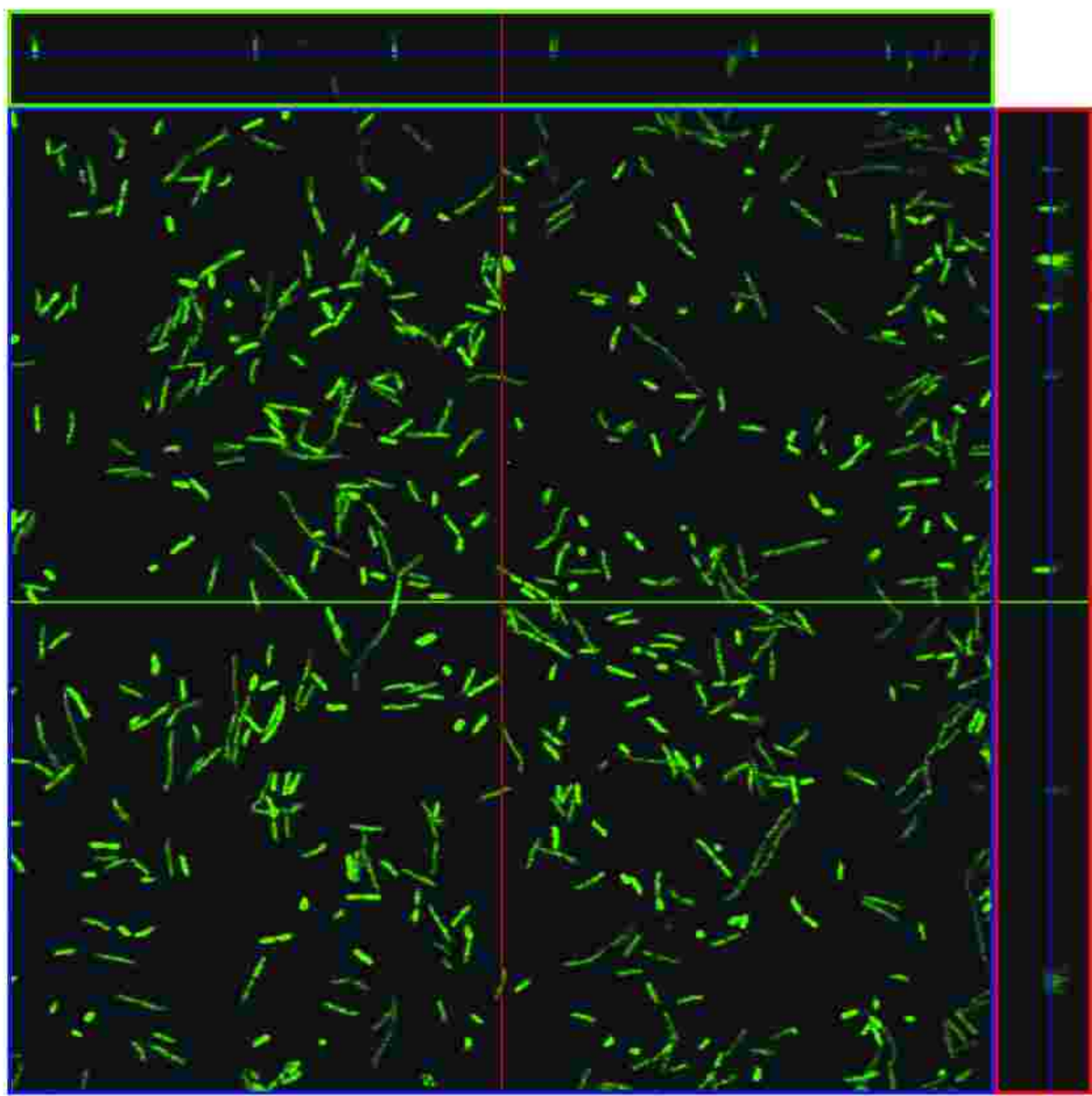


A


2.0
1.5
1.0
0.5
0.0
OD595
28ºC
37ºC
MS427pSU2718
MS427pFdeC

B


pFdeC


pSU2718